http://eprints.gla.ac.uk/143105/

Supramolecular polymer hydrogels induced by host-guest interactions with di-[cyclobis(paraquat-p-phenylene)] cross-linkers: from molecular complexation to viscoelastic properties

Matthieu Fumagalli[1,2], Khaled Belal[3], Hui Guo[1,2], François Stoffelbach[4],

Graeme Cooke,[5] Alba Marcellan[1,2], Patrice Woisel[3*] and Dominique Hourdet[1,2*]

[1]Laboratoire Sciences et Ingénierie de la Matière Molle, CNRS, ESPCI Paris,

PSL Research University, 10 rue Vauquelin, F-75005 Paris, France.

[2]Laboratoire Sciences et Ingénierie de la Matière Molle, Université Pierre et Marie Curie,

Sorbonne-Universités, 10 rue Vauquelin, F-75005 Paris, France.

[3]Unité des Matériaux et Transformations, UMR CNRS 8207, ENSCL

Equipe Ingénierie des Systèmes Polymères (ISP) 59655 Villeneuve d'Ascq Cedex (France).

[4]Sorbonne Universités, UPMC Univ Paris 06, CNRS, Institut Parisien de Chimie Moléculaire,

UMR 8232, Equipe: chimie des polymères, F-75252 Paris Cedex 05, France

[5] WestCHEM, School of Chemistry, University of Glasgow, Glasgow, G12 8QQ, UK

Email addresses:

matthieu.fumagalli@univ-lyon1.fr,   khaled.belal@ed.univ-lille1.fr,   hui.guo@espci.fr,

francois.stoffelbach@upmc.fr,   graeme.cooke@glasgow.ac.uk,   alba.marcellan@espci.fr,

patrice.woisel@ensc-lille.fr, dominique.hourdet@espci.fr

ABSTRACT

Supramolecular polymer networks have been designed on the basis of a π-electron donor/acceptor complex: naphthalene (N)/cyclobis(paraquat-*p*-phenylene) (CBPQT^{4+}=**B**). For this purpose, a copolymer of *N,N*-dimethylacrylamide **P(DMA-N1)**, lightly decorated with 1 mol% of naphthalene pendant groups, has been studied in semi-dilute un-entangled solution in the presence of di-CBPQT^{4+} (**BB**) crosslinker type molecules. While calorimetric experiments demonstrate the quantitative binding between N and B groups up to 60 °C, the introduction of **BB** crosslinkers into the polymer solution gives rise to gel formation above the overlap concentration. From a comprehensive investigation of viscoelastic properties, performed at different concentrations, host/guest stoichiometric ratios and temperatures, the supramolecular hydrogels are shown to follow a Maxwellian behavior with a strong correlation of the plateau modulus and the relaxation time with the effective amount of interchain cross-linkers and their dissociation dynamics, respectively. The calculation of the dissociation rate constant of the supramolecular complex, by extrapolation of the relaxation time of the network back to the beginning of the gel regime, is discussed in the framework of theoretical and experimental works on associating polymers.

INTRODUCTION

Today, solvent based technologies involving associating polymers are used in many fields due to their unique rheological properties, such as viscosifying, gelling, shear-thickening, and self-healing, which can further be controlled with environmental parameters such as temperature, pH, ionic strength, pressure and light [1-7]. This is typically the case of aqueous-based formulations that involve water-soluble associating polymers in a very broad range of technological areas such as enhanced oil recovery, paints and coatings, food additives, cosmetics and biomedical engineering [8-10]. In aqueous media, specific associations between macromolecular chains are generally enhanced with monomer units or sequences, called stickers, which usually interact through hydrogen bonds, hydrophobic and/or electrostatic interactions [7,11-12]. The simplified picture of these macromolecular assemblies is a semi-dilute solution of water soluble polymers that dynamically interact through microdomains or clusters. From this picture, the viscoelastic properties will depend on the number of clusters (physical cross-linkers), that are themselves dependent on the fraction of aggregated stickers and their aggregation number, as well as the life time of the stickers within the clusters. These critical parameters are generally controlled with the architecture of the polymer (e.g. telechelic, block, graft, star-like) including the number, distribution, size and chemical nature of associating units [2,3,13-15]. In the field of macromolecular assemblies, supramolecular chemistry has provided new methodology with highly specific, directional and reversible interactions, like hydrogen bonds, metal ligand or inclusion complexes [16-19]. Indeed, the supramolecular toolkit offers a wide range of binding strengths and dynamics that can be readily used to orchestrate macroscopic properties from the molecular level and the implementation of these binding motifs within polymer chains has paved the way to supramolecular polymer gels [20-23].

It is only during the last decade, that a specific attention has been paid to establish clear relationships between supramolecular interactions and viscoelastic properties of gels. Among these studies, the seminal work of Craig and co-workers who developed a systematic study based on the physical cross-linking of poly(vinylpyridine) with bimetallic pincers is particularly noteworthy [24-27]. This work, performed on organogels prepared in DMSO, highlight that the key parameters for the control of the viscoelastic properties of the network are the equilibrium association constant ($K_{eq} = k_a / k_d$) and the dissociation rate constant (k_d; k_a being the association rate constant), that are correlated to the fraction of metal-ligand complexes and their average life time ($\tau_0 = 1/k_d$). Although "strong means slow" is the central feature of the association process, there is not actually a strong consensus between viscoelastic properties and one of the few theories developed around transient and covalent networks [28-33]. This clearly remains an open question that needs to be addressed, particular with regard to concentration regimes. When dealing with supramolecular polymer assemblies in water, hydrogen bonding or metal complexation interactions have been successfully developed as in the case of methacryl-succinimidyl modified poly(N-isopropylacrylamide) [PNIPAM] [34], supramolecular poly(N,N,dimethylacrylamide) metallogels based on histidine−Nickel coordination bonds [35], bio-inspired complexes based on catechol-Fe^{3+} and histidine-Fe^{3+}, which also demonstrate pH-responsive properties [36-37], or supramolecular gels prepared from heterotelechelic associating polymers: PS-b-PNIPAM-terpyridine [38]. In these works, the authors try to correlate the dissociation time of the supramolecular bond to the relaxation time of the network (τ) that is interpreted as the time for the sticker exchange between junctions (τ_{ex}). It appears that in semi-dilute regime τ_0 is smaller than τ_{ex} and that the difference between the two time constants increases with gel concentration. Even though the sticker dissociation rate remains constant when the gel concentration varies, exchange of stickers is detected from rheological measurements only when a dissociated sticker finds and

combines with a new partner instead of associating with its old one. Such behavior has been initially proposed in the framework of the sticky Rouse model of Rubinstein and Semenov [31]. On their side, Craig et al. argue that the relaxation time of the supramolecular network can be identified with the intrinsic lifetime of the supramolecular bond when the polymer concentration reaches the sol/gel transition [25]. Host-guest complexes have also been widely used [19] with many examples of supramolecular networks involving cyclodextrin (CD) / adamantane (AD) complementary binding motifs [21,23,39-40]. For instance, the formation of transient networks has been described with complementary poly(sodium acrylate) chains carrying complementary CD or AD motifs [41-42] as well as with AD-modified PNIPA using CD-dimer as cross-linker [43]. Other host molecules have also been considered like the cucurbit[n]uril (CB[n]) family that are cyclic, methylene-linked oligomers of glycoluryl with a symmetric barrel shape [19,44]. When the cavity is sufficiently large, like CB[8], the host can accommodate two guests and act as physical cross-linker with water-soluble polymers carrying pendant methyl viologen or naphthoxy derivatives that behave as good first and second guest, respectively. From a detailed investigation performed with semi-dilute un-entangled solutions, Scherman and co-workers [45] have determined the guest dissociation rate constant from the viscoelastic properties of the gel following the procedure described by Craig and co-workers [25]. Moreover, they showed that the characteristic time of the supramolecular network increased linearly with the cross-link density as theoretically predicted by Jongschaap [32].

In the field of host/guest complexes, the tetracationic cyclophane cyclobis(paraquat-p-phenylene) (CBPQT^{4+}) host molecule, most commonly named blue box, has become an important building block for the design of both pseudorotaxane [46], rotaxane [47,48], catenane [49] architectures and supramolecular polymeric materials featuring machine-like functions and/or stimuli responsiveness properties. However, while many studies on the

development of CBPQT[4+] based (macro)molecular assemblies have been carried out in organic media [50,51], comparatively much less work has been devoted to the creation of controllable supramolecular systems of this type in aqueous media [52-54]. In this framework, the complex formation between the hydrophilic electro-deficient blue box molecule and hydrophobic electron-rich guest units like tetrathiafulvalene or naphthalene moieties, has been notably investigated in aqueous media in order to mediate responsive properties like molecular recognition, self-assembly, volume or color modifications triggered by redox [55] or other environmental parameters like temperature [56,57], pH [58,59] or ionic strength [54]. Nevertheless, although the complex formation between blue box and guest molecules has been extensively studied at the molecular level by calorimetry and spectroscopic studies, its ability to develop supramolecular polymer network has scarcely been reported so far [60] and structure/properties relationships between molecular associations and viscoelastic properties have not been established. To tackle this problem, a di-blue box host molecule (BB) has been designed and its ability to cross-link naphthalene pendant groups, randomly distributed along a poly(*N*,*N*-dimethylacrylamide) chain, was studied in semi-dilute un-entangled solutions (see **Figure 1**). From calorimetric, spectroscopic and viscoelastic experiments, the aim of the present work is to investigate the associating properties of these new supramolecular polymer hydrogels and to bridge the gap between molecular and macroscopic levels.
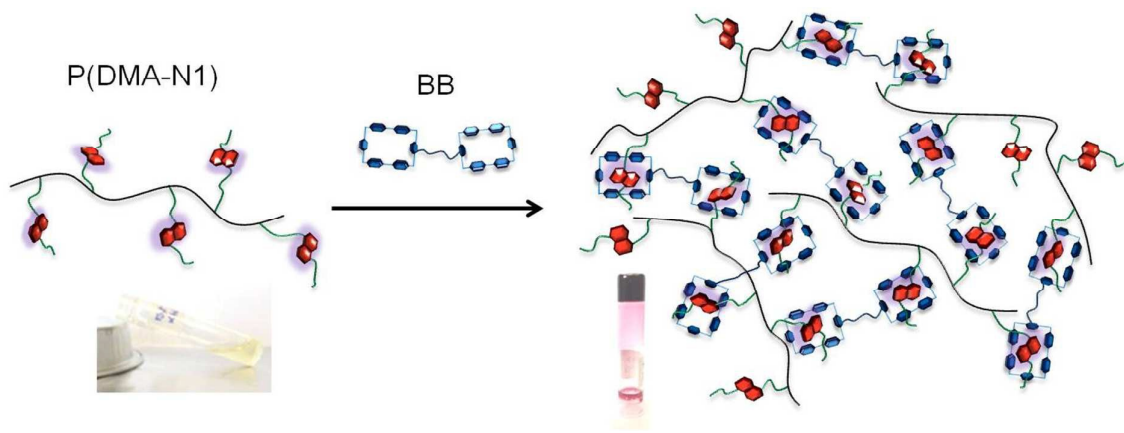

Figure 1. Formation of a supramolecular polymer network induced by host-guest interactions

between homoditopic tetracationic macrocycle cyclobis(paraquat-*p*-phenylene) (BB) and poly(*N,N*-dimethylacrylamide-co-naphthalene acrylamide) containing 1 mol% of naphthalene comonomer (P(DMA-N1)).

EXPERIMENTAL SECTION

Building Blocks. As shown in **Figure 1**, the formation of a supramolecular polymer network in aqueous media rests on host-guest interactions developed between two types of building blocks: a naphthalene functionalized side-chain copolymer P(DMA-N1) and a supramolecular crosslinker featuring two CBPQT^{4+} moieties (BB). This homoditopic tetracationic macrocycle cyclobis(paraquat-p-phenylene) host molecule was obtained by coupling two CBPQT^{4+} (B) units carrying an alkyne end group with 1,6-hexanediazide according to a Huisgen cycloaddition as already described in a previous paper [60]. The water-soluble guest copolymer, P(DMA-N1), was obtained by RAFT copolymerization of *N,N*-dimethylacrylamide with an acrylamide comonomer functionalized with a lateral naphthalene group (see Supporting Information with **Figures S1 to S5**). It is characterized by a number average degree of polymerization DP$_n$≅1100 (Đ =1.25) and a low molar content of naphthalene groups (1 mol%); i.e. an average of $N_n \cong$ 10-11 naphthalene groups per polymer chain. In the following, naphthalene groups will be named N while B and BB will symbolize mono-blue box and di-blue box molecules, respectively.

Nuclear Magnetic Resonance (NMR). Host/guest complexes were studied by ^{1}H NMR and compared with their precursors. Experiments were carried out on a Bruker Avance spectrometer operating at 300 MHz in D$_2$O with 5 mm broadband probe.

UV-Vis spectroscopy. The complex formation and its temperature dependence were characterized by UV-Vis spectroscopy using a Varian Cary 50 Scan equipped with a single cell Peltier temperature controller.

Isothermal Titration Calorimetry (ITC).

The formation of blue box (**B**) complexes was studied at fixed temperature, 20 °C or 60 °C, using a nano-ITC titration calorimeter from TA Instruments following standard procedures. The sample cell (1 mL) was initially filled with naphthalene derivatives (molecule or

polymers), or water (for dilution measurements), while the blue box (**B**) solution was introduced into a 250 μL injection syringe. The titration was carried out by a step-by-step injection of the **B** solution into the sample cell under continuous stirring (400 rpm). A similar procedure was carried out at 25 °C for the titration of **P(DMA-N1)** with di-blue box (**BB**) using a MicroCal VP-ITC titration calorimeter from Malvern with a sample cell volume of 1.42 mL and a 300 μL injection syringe. The enthalpy of complexation (ΔH) was obtained after subtraction of the dilution curve from the titration one. The binding constant (K_a), as well as other thermodynamic parameters including free energy (ΔG) and entropy (ΔS), were obtained after data fitting using a single set of identical sites.

Low shear viscosity. Newtonian viscosity of dilute and semi-dilute copolymer solutions were determined from low shear experiments carried out at T = 20 °C with a Contraves LS30 viscometer.

Rheology. The viscoelastic properties of copolymer solutions were studied in the semi-dilute regime, using a stress-controlled rheometer (AR 1000 from TA Instruments) equipped with a cone/plate geometry (diameter 40 mm, angle 2, truncature 55.9 μm). The experiments were performed in the linear viscoelastic regime that was established for each sample by a stress sweep at the lowest frequency. For most of the studies, the shear stress was set at 2 Pa and a frequency sweep was applied between 0.01 and 100 Hz at a given temperature accurately controlled with a high-power Peltier system. A particular care was taken to avoid the drying of the sample by using a homemade cover that prevents water evaporation during the experiments. In these conditions, the frequency dependence of dynamic moduli (G' and G") as well as complex viscosity (η^*) were recorded at various temperatures, typically 5, 15, 25 and 35 °C. For polymer solutions, the viscosity plateau observed in the low frequency range and defined as the Newtonian viscosity was also used to complement previous values obtained from low shear experiments.

RESULTS AND DISCUSSION

Host-Guest interactions. The association process taking place in water between host and guest molecules has been first investigated using UV-Vis spectroscopy and ITC.

Monitoring complexation by UV-Vis spectroscopy.

We have first investigated the capability of **B** units to bind pendant naphthalene groups of **P(DMA-N1)** by UV-Vis spectroscopy. For that purpose, a spectroscopic titration of a **P(DMA-N1)** solution (1mM in N groups) was carried out by adding increasing amounts of an aqueous solution of **B**. As shown in **Figure 2**, the resulting complex gives rise to an optical absorption band centered around $\lambda_{max} = 525$ nm, characteristic of B/N type complexes.
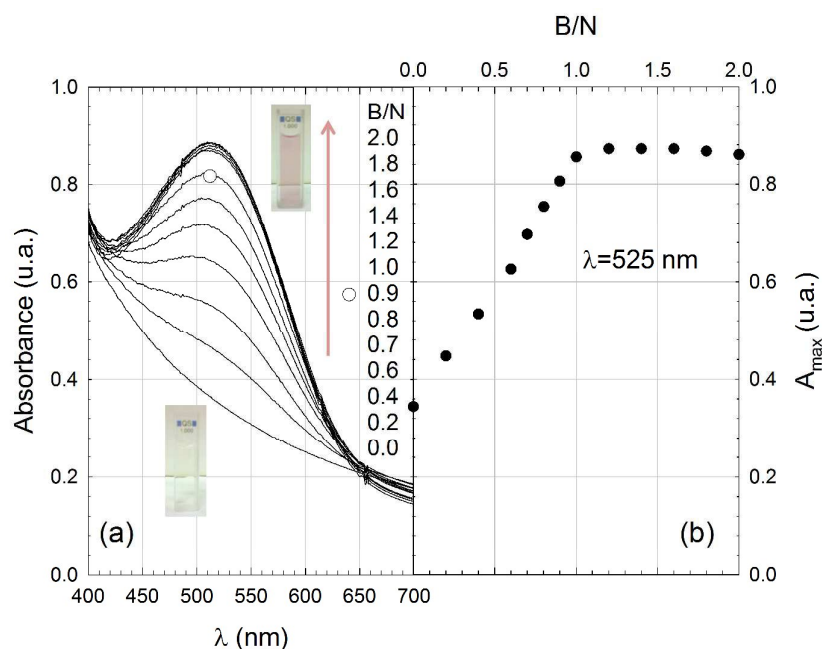

Figure 2. (a) Spectroscopic titration of an aqueous solution of **P(DMA-N1)** ([N]=1 mM) with a B solution ([B] = 30 mM); T = 20 °C.
(b) Absorption maximum (λ=525 nm) versus the stoichiometric ratio (B/N).

The intensity of the charge-transfer band increases with increasing amounts of added **B** and finally levels off for a molar ratio **P(DMA-N1)/B** of 10 that roughly corresponds to the complex stoichiometry; i.e. one **B** per Naphthalene group (B/N=1). As shown in **Figure S6**,

(Supplementary Information), the intensity of the absorption band decreases with temperature, demonstrating qualitatively that the strength of the complex decreases during heating. Although qualitative, this study clearly emphasizes that the complex is relatively strong as the absorption band still exists at very high temperature (T=75 °C) and is fully reversible within the time scale of the experiment as the original absorbance is recovered after a heating/cooling cycle.

Relative content of complexed units by Isothermal Titration Calorimetry.

More quantitative information can be retrieved from ITC experiments that allow simultaneous access to the average stoichiometry of the complex (B/N), as well as thermodynamic parameters like the binding constant (K_a), ΔG, ΔH and ΔS related to the following equations:

$$\text{N} + \text{B} \leftrightarrows \text{NB} \text{ with } K_a = \frac{[NB]_{eq}}{[N]_{eq}[B]_{eq}} \quad \{1\} \quad \text{and} \quad \Delta G = \Delta H - T\Delta S = -RTLnK_a \quad \{2\}$$

$$\text{with} \quad LnK_a = LnK_{T_{ref}} + \frac{\Delta H}{R}\left(\frac{1}{T_{ref}} - \frac{1}{T}\right) \quad \{3\}$$

where $[N]_{eq}$, $[B]_{eq}$ and $[NB]_{eq}$ are the equilibrium concentrations of naphtalene groups, uncomplexed and complexed blue box molecules, respectively.

A typical ITC experiment is given in **Figure 3** with the titration in water of a **P(DMA-N1)** solution with a concentrated solution of **B**. The enthalpograms obtained at T=20 °C (**Figure 3**) and T=60 °C (see **Figure S7** in Supporting Information) display a sharp exothermic titration profile with $\Delta H \cong$ -54 kJ/mol and a stoichiometric ratio of 9.5 CBPQT^{4+} molecules per **P(DMA-N1)** chain, that matches well with the host/guest stoichiometric ratio B/N of 1 previously estimated by UV-Vis spectroscopy.
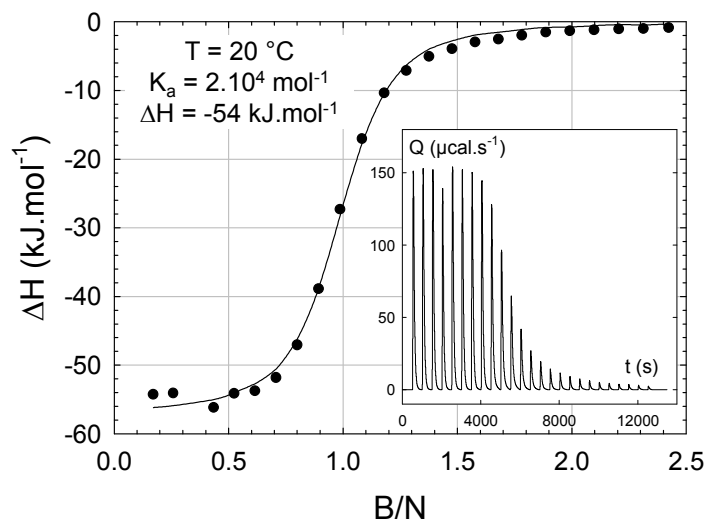
Figure 3. Isothermal calorimetric titration (T=20 °C) of a P(DMA-N1) aqueous solution ([N]=0.4 mM) with B ([B]=30 mM).

At 20 °C the association constant is relatively high (K_a=2.10^4 M^{-1}) but two orders of magnitude lower than the one obtained for the molecular complex CBPQT^{4+}/1,5-dialkyloxyNaphthalene (devoid of polymer chain) [52]. This large difference clearly highlights the impact of the structure and likely the degree of freedom of guest entities covalently attached to the macromolecular backbone. A similar behavior has been reported by Prud'homme and coworkers for the complex formation between poly(sodium acrylate) modified either with β-cyclodextrin or adamantyl groups [42]. When the calorimetric titration is carried out at higher temperature (T=60 °C; see **Figure S7** in Supporting Information), the complexation enthalpy remains almost unchaged (ΔH ≅ -55 kJ/mol) while the association constant falls by a factor ten to K_a≅1.4 x 10^3 M^{-1}, meaning that the number of (NB) complexes also decreases (see equation {1}). This result is in good agreement with our previous UV-Vis observations, and the evolution of K_a as a function of the temperature (**Figure S8** given in supporting information) can be readily evaluated through the Van't Hoff law (see equation {3}) considering a constant complexation enthalpy over the temperature range.

For a similar ITC experiment, performed with **BB** crosslinkers at T=25 °C (see **Figure S9** in Supporting Information), the thermodynamic parameters remain very close to those extrapolated at the same temperature with **B***: ΔH=-52 kJ/mol (ΔH*=-54 kJ/mol), ΔS=-99 J.mol^{-1}K^{-1} (ΔS*=-102 J.mol^{-1}K^{-1}) and K_a=9800 M^{-1} (K_a*=13800 M^{-1}). For this reason, we will assume in the following that the equilibrium constants relative to the formation of the mono-coordinated complex (K_1) and di-coordinated complex (K_2) are similar: $K_1 = K_2 = k_{as}/k_{dis}$ {4}, k_{as} and k_{dis} being the rate constants for NB association and dissociation, respectively,

$$\text{with} \quad K_1 = \frac{[NBB]_{eq}}{[N]_{eq}[BB]_{eq}} \quad \text{corresponding to} \quad N + BB \leftrightarrows NBB \quad \{5\},$$

$$K_2 = \frac{[NBBN]_{eq}}{[N]_{eq}[NBB]_{eq}} \quad \text{corresponding to} \quad NBB + N \leftrightarrows NBBN \quad \{6\},$$

[N]$_{eq}$, [BB]$_{eq}$, [NBB]$_{eq}$ and [NBBN]$_{eq}$ being the equilibrium concentrations of naphtalene groups, uncomplexed di-blue box molecules, mono- and di-coordinated blue box, respectively.

From these equilibrium, and using the equations (S5-13) developed in the Supporting Information, it is possible to calculate, for each experimental conditions, the relative fractions of N species at equilibrium that are distributed in free naphthalene [N]$_{eq}$, monocomplexed diblue box [NBB]$_{eq}$ and dicomplexed diblue box [NBBN]$_{eq}$. From these equations, the molar fractions of N species at equilibrium have been plotted in **Figure 4a** versus the initial concentration of naphthalene *[N]$_T$*, assuming stoichiometric conditions : *[N]$_T$=[B]$_T$*.
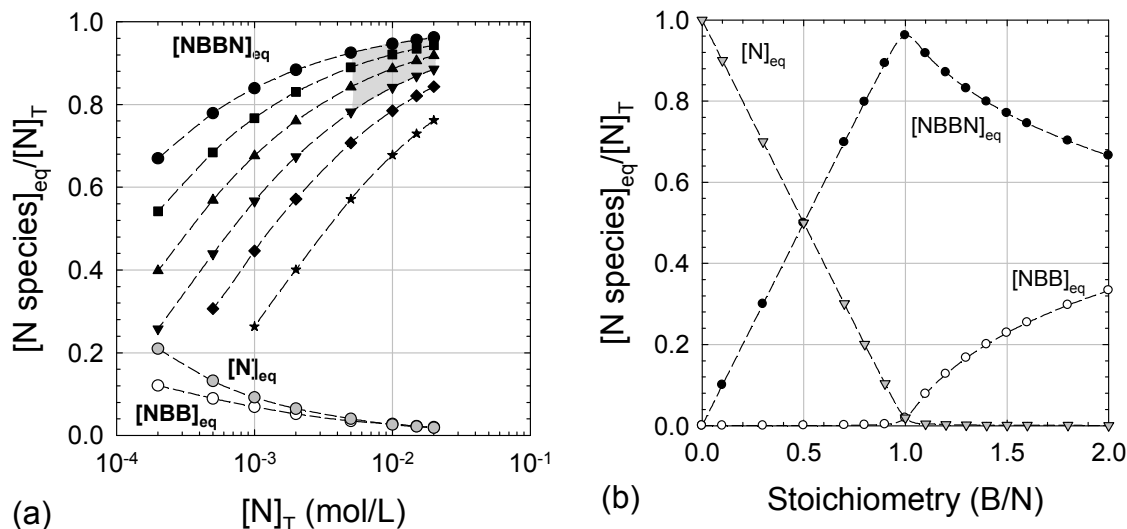
Figure 4. Calculated molar fractions of N species at equilibrium in the case of the complex formation between **P(DMA-N1)*** and **BB**. **(a)** Concentration and temperature dependences of N species in stoichiometric conditions ($[B]_T = [N]_T$) with: $[N]_{eq}$ at T=5°C (●),$[NBB]_{eq}$ at T=5°C (○) and $[NBBN]_{eq}$ at T=5°C (●), 15°C (■), 25 °C (▲), 35 °C (▼), 45 °C (◆) and 60 °C (★).The gray zone delimits the area of interest where supramolecular hydrogels will be studied. **(b)** Variation of N species at T=5 °C as a function of stoichiometry for a fixed concentration of naphthalene : $[N]_T = 0.02$ M ($C_p \cong 20$ wt%).
*With this copolymer, the conversion between the total molar concentration of Naphthalene ($[N]_T$ in mol/L) and the polymer concentration is C_p (wt%) $\cong 10.[N]_T$.

At T=5 °C, temperature at which the association constant is high (K_a=66 000 M^{-1} as determined from Van't Hoff law plotted in **Figure S8**), the complex formation strongly increases with the concentration of naphthalene and di-blue box molecules. For *[N]$_T$* > 0.05 M, which corresponds roughly to the concentration of viscoelastic gels that will be studied later on ([P(DMA-N1)] > 5 wt%), the complex formation is quite effective with more than 90 % of N groups embedded into di-coordinated complexes (NBBN), thereby indicating the potential of BB to act as an effective cross-linking agent. On the same **Figure 4a**, we can also notice that the temperature strongly affects the relative fractions of N species with a decrease of NBBN complexes that still represent more than 50 % at 60 °C for *[N]$_T$* >0.005 M. As shown in **Figure 4a**, the gray zone delimits the area where the supramolecular hydrogels will

be studied. This is the domain where the fraction of di-coordinated complexes will be higher than 80 %, and more generally higher than 90 %.

In **Figure 4b** the molar ratio B/N is varied at low temperature (T=5 °C), when the complex formation is quite strong, and for a given naphthalene concentration ($[N]_T$=0.02 M). Under these conditions, the continuous addition of **BB** gives rise mainly to the formation of NBBN complexes that reach their maximum number at the stoichiometry: p_{NBBN}=[NBBN]$_{eq}$/$[N]_T$=96 % (B/N=1). Above these conditions, the number of di-coordinated complexes progressively decreases to the benefit of mono-coordinated complexes.

These quantitative data are also well supported by ^{1}H NMR experiments performed with polymer formulations prepared with different stoichiometric ratios: B/N=0.5, 1 and 1.5 (see **Figure S11** in Supporting Information). In this case, the analysis of ^{1}H chemical shifts belonging to either free or complexed molecules qualitatively demonstrate that at rather relatively high concentration ($[N]_T \cong 0.01$ M) and moderate temperature (T=20 °C), the fraction of uncomplexed naphthalene and blue box molecules are negligible under stoichiometric conditions. More generally, this information regarding the distribution of naphthalene groups between complexed and uncomplexed forms will be useful to understand the viscoelastic properties as this distribution will directly impact the formation of physical crosslinks and elastically active chains.

Supramolecular polymer networks

Considering the molecular information obtained previously on the complex formation between naphthalene side-chains and blue box molecules, we will investigate now how these host/guest interactions control the formation and the properties of supramolecular hydrogels.

Concentration regimes.

Prior to viscoelastic analysis of host-guest supra-macromolecular assemblies, the Newtonian viscosity of the copolymer **P(DMA-N1)**, which will be central in this study, has been investigated in pure water. As plotted in **Figure 5**, the concentration dependence of the specific viscosity (η_{sp}) clearly displays two different regimes from either side of $C_p{}^*$=2 wt%.
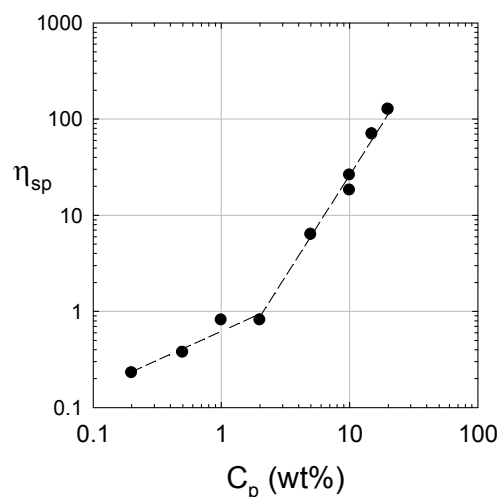

Figure 5

Concentration dependence of the specific viscosity (η_{sp}) of aqueous solutions of **P(DMA-N1)** at T=25 °C.
The log-log plot of $\eta_{sp}\sim C^\alpha$ gives $\alpha\cong0.6$ for $C_p\leq2$ wt% and $\alpha\cong2.1$ for $2\leq C_p\leq20$ wt%.

This overlap concentration, that defines the border between dilute and semi-dilute regimes, is in good agreement with other criteria such as $C_p{}^* \cong 1/[\eta] \cong 2$ wt% (with $[\eta] = 44$ mL/g) or $\eta_{sp} \cong 1$ at $C_p{}^*$ [61]. Similarly, the theoretical exponents of the scaling relation $\eta_{sp} \sim C_p{}^\alpha$ are close to the theoretical values of 1, expected in the dilute regime, and 2 for the semi-dilute un-entangled regime in Θ-solvent. Generally, the entangled regime is reached at significantly higher concentration, typically around $C_e \cong 5\text{-}10.C_p{}^*$ and with much higher exponent for the scaling relation $\eta_{sp} \sim C^\alpha$ (α=14/3 in Θ-conditions) [61]. Consequently, we will assume that the entangled regime mainly starts close or above 20 wt% and that all the following experiments performed at $5 < C_p \leq 20$ wt% will correspond to the semi-dilute un-entangled regime.

Polymer assemblies

Considering the distribution of naphthalene groups between complexed and uncomplexed forms, as well as the regime of polymer concentration, one can expect that the complex formation between naphthalene pendant groups and **BB** molecules will lead to polymer assemblies with a very broad range of viscoelastic properties. As shown in **Figure 6**, there are 3 different coordination states for the di-blue box molecules (BB, N-BB and N-BB-N), that can be calculated from the equilibrium constants, and then 4 different states of association regarding the naphthalene groups: N and N-BB dangling groups, N-BB-N intra-chain bound and N-BB-N inter-bound, where only the last one is elastically active. The viscoelastic behavior of such assemblies is investigated in the following section with a series of formulations where the key parameters are: the polymer concentration, the host-guest ratio, the temperature and the molar mass.
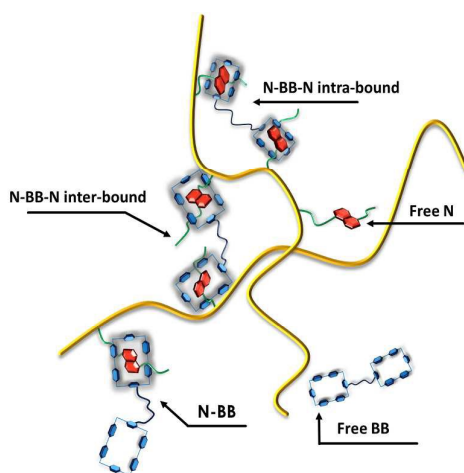
Figure 6

Schematic representation of supramolecular assemblies in semi-dilute solutions with four different states of association for pendant N groups and BB cross-linkers:
free N, free BB, mono-coordinate N-BB and di-coordinate N-BB-N with intra- or inter-chain association.

Influence of polymer concentration and host-guest ratio.

A first set of rheological experiments was carried out by working at 5 °C, with a fixed polymer concentration (C_p=10 wt%), by adding increasing amount of supramolecular cross-

linker **BB** (see **Figure 7a**). Starting with a purely viscous solution, the introduction of **BB** effectively promotes the formation of interchain associations leading to a huge increase of the Newtonian viscosity. The highest viscosity is obtained around the optimal stoichiometry, when a maximum number of **BB** are able to form duplex interactions with pendant naphthalene groups (N-BB-N). Below this stoichiometry most of BB are involved in di-coordinate complexes but their number are limited by the amount of added **BB**. Above the optimal stoichiometry, there is an increasing number of mono-coordinate complexes (N-BB) that will not participate to the network connectivity (see **Figure 7b**).
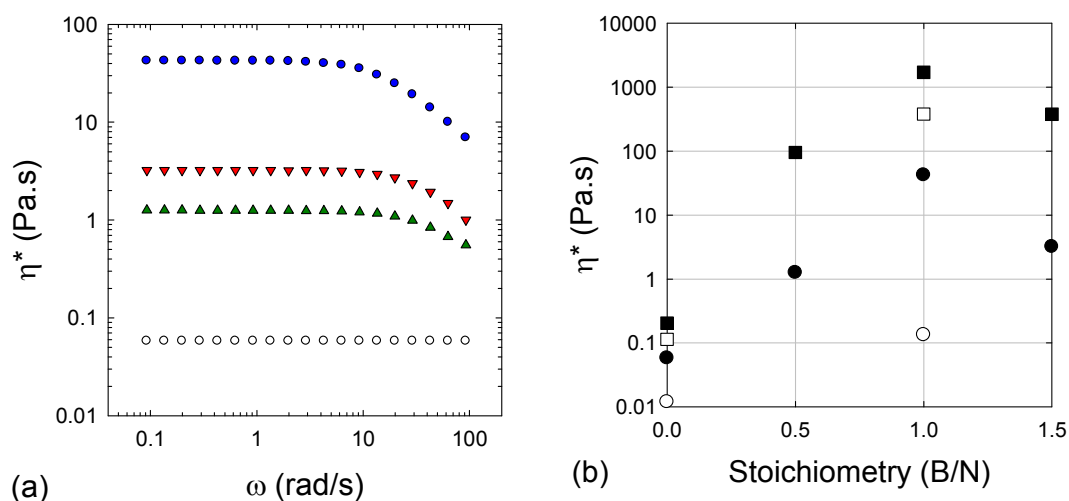
Figure 7. (a) Variation of the complex viscosity of a **P(DMA-N1)** solution (C_p=10 wt%) with various amounts of added **BB**: B/N=0 ($\bigcirc$); 0.5 ($\blacktriangle$); 1 ($\bullet$) and 1.5 ($\blacktriangledown$); T=5 °C. **(b)** Variation of the Newtonian viscosity of **P(DMA-N1)** solutions with host-guest stoichiometry: C_p (wt%)=5 ($\bigcirc$), 10 ($\bullet$); 15 ($\square$) and 20 ($\blacksquare$); T=5 °C.

The properties of supra-macromolecular assemblies are highlighted in **Figure 8a** where viscoelastic moduli are plotted against frequency for three different formulations (C_p=10 wt %) prepared at different stoichiometries: B/N=0.5, 1 and 1.5. As described previously, the best network properties are obtained in stoichiometric conditions with a typical Maxwellian behavior characterized by a plateau modulus (G_0= 612 Pa) and a single relaxation time defined by the opposite of the crossover frequency: $\tau=(\omega_c)^{-1}$=0.07 s.

Figure 8. (a) Variation of storage modulus (hollow symbols) and loss modulus (filled symbols) of **P(DMA-N1)** solutions (C_p=10 wt% (left) and 20 wt% (right)) at T=5 °C as a function of added BB: B/N=0.5 (△▲); 1 (○,●) and 1.5 (▽▼).
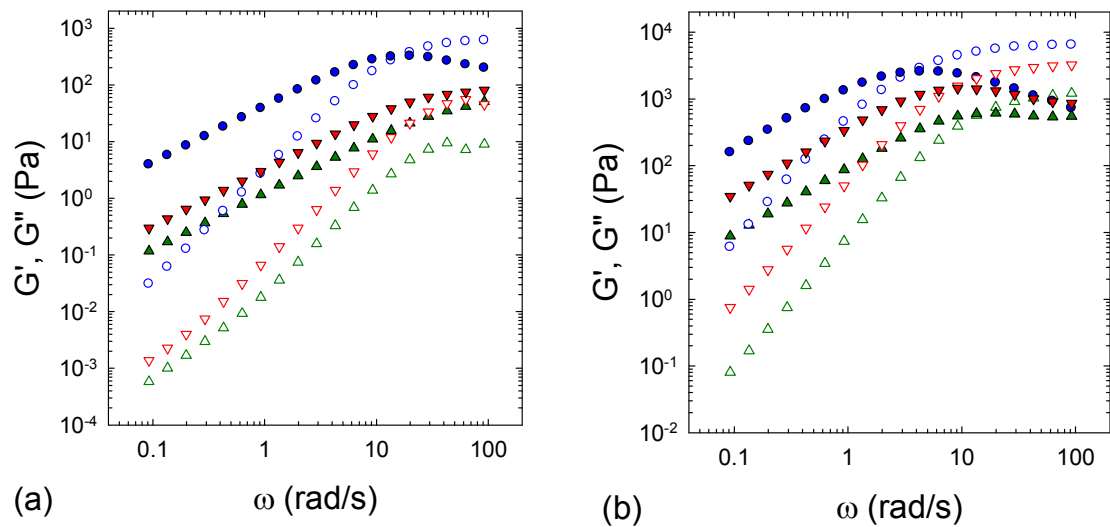
The corresponding picture is that the supramolecular polymer network responds to the stress applied by the rheometer by relaxing back to the equilibrium at a rate β that is the reciprocal of the relaxation time: $\beta=\omega_c=1/\tau$. Consequently, at very low frequency ($\omega<<\beta$), the system behaves like a viscous fluid (G''>G') as the physically crosslinked polymer chains relax faster than the experimental time scale. In these conditions the solution is Newtonian and the viscosity is given by $\eta=G_0.\tau$=43 Pa.s. Conversely, at high frequency ($\omega>>\beta$) the physical cross-linkers are active and the system shows an elastic behavior with a plateau modulus proportional to the density of elastically active chains. When moving away from the stoichiometric conditions (see B/N=0.5 and 1.5 on **Figure 8a**) the macromolecular assembly is no longer elastic in the frequency range explored as the relaxation rate of polymer chains increases with decreasing number of efficient cross-links.

The same holds for the solutions prepared at higher polymer concentration (C_p=20 wt% in **Figure 8b**) but in this case all the formulations prepared with B/N=0.5, 1 and 1.5, display a viscoelastic behavior in the frequency window due to the higher level of physical cross-

linking. Nevertheless, we clearly observe for all the polymer solutions prepared in the semi-dilute regime, a decrease of the Newtonian viscosity (see **Figure 7b**), the plateau modulus and the relaxation time when moving away from the stoichiometry (see **Table 1**). While the stoichiometry strongly influences the viscoelastic properties of the supra-macromolecular network, the same holds with the polymer concentration. Indeed, in stoichiometric conditions, all the formulations prepared at $C_p \geq 10$ wt% display a Maxwellian behavior (see **Figure S12** in Supporting Information) with a plateau modulus and a single relaxation time that increase with increasing concentration. The variation of the relaxation time with polymer concentration and stoichiometry (see **Table 1**) can be related to the variation of the effective number of physical cross-links per chain (increasing number of inter-chain associations and elastically active sub-chains per macromolecule) as we will discuss later. Similarly, as G_0 scales with the density number of elastically active chains, an increase of G_0 is naturally expected when the mean number of elastic sub-chains is increased either by increasing the polymer concentration or the fraction of di-coordinate N-BB-N that depends on the B/N ratio.

Table 1. Viscoelastic parameters obtained at T=5 °C for **P(DMA-N1)** at various polymer concentrations (C_p) and host/guest stoichiometry (B/N). The Newtonian viscosities of polymer solutions without added **BB** (B/N=0) were extrapolated at 5 °C from the values determined at 25 °C and assuming an Arrhenius behavior $\eta = A \exp(E_\eta / RT)$ with an activation energy E_η=23 kJ/mol as determined for C_p=10 wt% (see **Figure 9**).

C wt%	B/N=0	B/N=0.5			B/N=1.0			B/N=1.5		
	η Pa.s	G_0 Pa	τ s	η Pa.s	G_0 Pa	τ s	η Pa.s	G_0 Pa	τ s	η Pa.s
5	0.012						0.134			
10	0.058			1.26	612	0.069	42.4			3.22
15	0.114				2600	0.146	379			
20	0.204	1274	0.075	95.5	6600	0.259	1710	3300	0.115	378

In these stoichiometric conditions, the elastic properties dramatically drop below C_p=10 wt%. At C_p=5 wt% for instance, the viscosity of the solution increases 10 times with added **BB** but there is no elastic behavior (G''>G') in the frequency window explored (see **Figure 7b** and **Table 1**). Accordingly, we will consider that the gelation threshold, where the cross-link

density becomes high enough to induce the formation of a percolated network, occurs within this range: C_p=5-10 wt%.

Influence of temperature

In the case of physical assemblies, where dynamic properties are strongly correlated to the lifetime of supramolecular associations, the dissociation rate of molecular stickers remains very sensitive to environmental conditions. This is the case for the solvent medium, as nicely demonstrated by Craig and co-workers with poly(4-vinylpyridine) and bis-Pd(II) organometallic cross-linkers [25], but temperature is of course a very simple parameter that can be used to tune the level of interactions. According to the thermodynamic properties of the stickers, temperature can be used to trigger responsive assemblies by heating for systems involving LCST moieties but more generally an increase of temperature is known to weaken the binding energy like with Van der Waals, hydrogen bonding or metal/ligand interactions [5,20]. In the case of supramolecular interactions between blue box and naphthalene derivatives, we have seen previously that the association constant was strongly decreased between 20 and 60 °C from K_a= 20 000 to 1400 M^{-1}. In the case of the stoichiometric formulation (C_p=20 wt%, $[N]_T$=$[B]_T \cong 0.02$ M), the viscoelastic properties are mainly shifted along the x-axis towards higher frequency (lower relaxation time) when the temperature is increased from 5 to 35 °C and a time temperature superposition of these experiments is given in **Figure 9a** where the dynamic moduli are plotted versus the reduced frequency: ω/ω_c. First of all, we can consider that in this range of temperature, the weak dependence of the elastic modulus is in good agreement with the temperature dependence of the equilibrium constant as it was shown that the fraction of di-coordinated complexes (N-BB-N) only weakly decreases from 96 to 88 % between 5 to 35 °C (see **Figure 4a**). Things are different at high temperatures, above 60 °C for instance, but in this case there is no way to determine the plateau modulus as the formulation is almost liquid in the frequency range explored.

Assuming that the elastic modulus remains almost constant between 5 and 35°C, this means that the variation of the elastic properties of the supramolecular polymer network with temperature is mainly controlled by the dissociation rate of the stickers that becomes faster with increasing temperature.
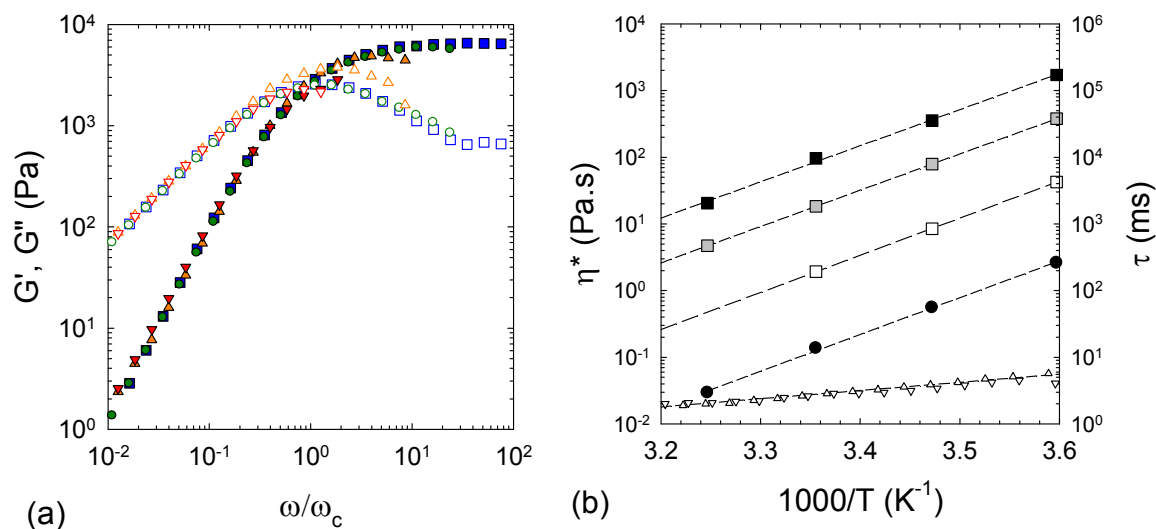

Figure 9. Temperature dependence of viscoelastic properties of **P(DMA-N1)** supramolecular assemblies prepared in stoichiometric conditions (B/N=1). **(a)** Master curve of G' (filled symbols) and G'' (hollow symbols) for $C_p = 20$ wt% with T=5 °C (■□), 15 °C (●○), 25 °C (▲△) and 35 °C (▼▽). **(b)** Arrhenius plots of Newtonian viscosity (square) and relaxation time (circle) for stoichiometric formulations prepared at $C_p = 10$ wt% (□), 15 wt% (■) and 20 wt% (■●). The Arrhenius plot of the viscosity measured at C_p=10 wt% without added **BB** (B/N=0 △) and with stoichiometric amount of mono-blue Box (▽) are given for comparison.

Using the relaxation time and/or the Newtonian viscosity obtained between 5 and 35 °C, we can get the activation energy (E_η or E_τ) of the relaxation process by considering an Arrhenius variation of the dynamic parameters. As we can see from **Figure 9b**, the stoichiometric formulation (C_p=20 wt%, B/N=1) shows straight lines for the log-log plots of τ and η with similar slopes close to 105 kJ/mol (see also **Table 2**). Again this common behavior between η and τ emphasizes that the elastic modulus obtained at high frequency ($\omega/\omega_c \gg 1$) does not vary substantially with the temperature. From the Arrhenius treatment performed on various formulations (see **Figure 9b** and **Table 2**) we can notice that the activation energy is almost

constant ($E_a \cong 105$ kJ/mol) and maximum in stoichiometric conditions within the concentration range C_p=10 to 20 wt%. This value, close to $40 k_B T$ at room temperature, is quite high and comparable with activation energies reported with other supramolecular assemblies [35,62] or with hydrophobically modified water-soluble polymers with long alkyl stickers like C20 [2].

Table 2. Activation energies of P(DMA-N1) formulations prepared with added di-blue box. C_p is the polymer concentration, B/N the stoichiometric ratio, E_η and E_τ the activation energies calculated from the Arrhenius dependence of the Newtonian viscosity (η) and the relaxation time (τ).

C_p wt%	5	10				15	20		
B/N	1	0	0.5	1	1.5	1	0.5	1	1.5
E_η (E_τ) kJ/mol	45	23.2	67.6	106.6	75.3	104	86.6	103.6 (105.6)	91.4

The fact that this activation energy does not really depend on the concentration for stoichiometric gels means that, in these conditions, the relaxation rate is mainly dominated by the dissociation rate of the stickers. For concentrations below the gelation threshold (C_p=5 wt%, B/N=1), or when deviating from the stoichiometric conditions (B/N=0.5 or 1.5; see **Table 2**), the activation energy decreases progressively towards the value relative to the polymer relaxation itself. As shown in **Figure 9b**, this limit value ($E_{a,pol}$=23 kJ/mol) is reached in absence of supramolecular cross-linkers (B/N=0) or with a stoichiometric addition of **B** that does not modify the rheological properties. As the activation energy of the supramolecular polymer network (E_a) comprises two contributions [62], the energy of activation for the breakage of the supramolecular bonds ($E_{a,dis}$) can be obtained by subtracting the energy of activation for the polymer relaxation ($E_{a,pol}$): $E_{a,dis} = E_a - E_{a,pol} \cong 105 - 23 = 82$ kJ/mol. The physical picture of thermally activated bond dissociation in supramolecular polymer networks is illustrated in **Figure 10** with $E_{a,as}$ the energy of activation for the complex formation and ΔH the enthalpy of complex formation figuring the binding energy (E_b): $\left| \Delta H \right| \cong E_b = E_{a,dis} - E_{a,as}$. The quantitative comparison with the enthalpy, previously determined by ITC ($\left| \Delta H \right|$=52 kJ/mol), would suggest a relatively high energy barrier for the

complex formation ($E_{a,as} \cong 30$ kJ/mol) that can be related to the entropic loss of bringing the naphthalene and the blue box together and to the macromolecular rearrangement to preconfigure the motifs for complex formation.
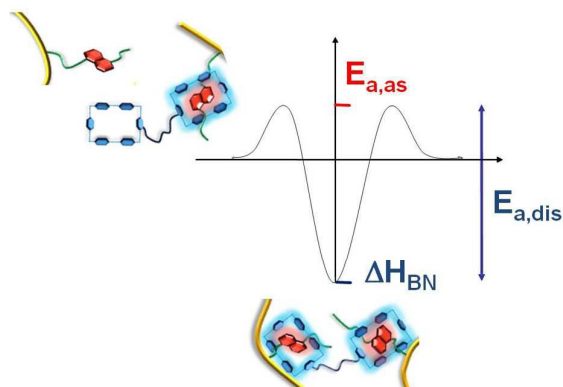

Figure 10

Energy profile for reversible host-guest complex formation in supramolecular polymer network.

Nevertheless, as theoretically described by Rubinstein and Semenov for solutions of associating polymers [63], a network strand can break and recombine again many times at the same pair of stickers until at least one of them finds a new partner. Although a bond would typically break after a time $\tau_b \propto \exp\left[(E_b + E_{a,as})/RT\right]$ {7}, the effective lifetime of the bond undergoing the recombination process (τ_b^*) is therefore larger as well as the apparent activation energy. For instance, the theory predicts a higher contribution for the binding energy in the gel regime ($\tau_b^* \propto \exp\left[(1.5E_b + E_{a,as})/RT\right]$) that implies a much lower energy barrier for the complex formation ($E_{a,as} \cong 5$ kJ/mol). This small energy can be compared to experimental values determined by stopped-flow experiments in the case of supramolecular hydrogels formed with cucurbit[8]uril and dimethyl viologen ($E_{a,as} \cong 10$ kJ/mol) [64]. Even if we cannot really conclude in the present study, especially on the quantitative value of the energetic barrier to association ($E_{a,as}$), these characteristic energies are very important features to consider for the design of supramolecular hydrogels as $E_{a,dis}$ determines the mechanical strength, whereas $E_{a,as}$ accounts for the capacity of the materials to self-heal [64].

Network formation and structure

From the previous results, it can be seen that the connectivity and consequently the elastic modulus of the supramolecular polymer network is mainly determined by the copolymer concentration and the host/guest stoichiometric ratio. On the other hand, the relaxation time of the network mainly depends on the dissociation rate of supramolecular interactions and number of effective cross-linkers. A schematic representation of supra-macromolecular assemblies has been given in **Figure 6**.

In order to give a more quantitative description of these assemblies, we will use the data obtained at high frequencies that characterize the elastic network when supramolecular crosslinks are active on this timescale. As we are working in the semi-dilute un-entangled regime, we will consider that the elastic modulus G_0 is mainly determined by the interchain cross-linkers (see **Figure 6**) and consequently it will be used to calculate the number of elastically active chains. As suggested by Craig and co-workers [27], the phantom network model is more appropriate for the description of such assemblies with reversible cross-linkers and in this case the molar concentration of elastically active chains (ν in mol/m^3) is given by:

$$\nu = \frac{G_0}{RT(1 - 2/f)} \qquad \{8\}$$

where R is the gas constant, T the temperature and f the functionality of the crosslinks that is $f=4$ in the present system.

Starting with this molar concentration, we are then able to calculate:

1) the fraction of elastically active chains (f_x) by dividing ν by the total molar concentration of subchains (n_s); a subchain being a polymer sequence between two consecutive naphthalene units:

$$f_x = \frac{\nu}{n_s} = \frac{\nu}{C_p/M_{n,s}} \qquad \{9\}$$

2) the mean number of elastically active chains per copolymer chain (x) by dividing ν by the molar concentration of polymer chains (n_p):

$$x = \frac{\nu}{n_P} = \frac{\nu}{C_p / M_{n,p}} \quad \{10\}$$

3) the mean number of cross-links per copolymer chain:

$$N_x = x + 1 \quad \{11\}$$

and 4) the fraction of interchain bonds:

$$p_{inter} = N_x / N_n \quad \{12\}$$

with C_p the copolymer concentration (here in kg/m^3), $N_n \cong 10$ the total number of naphthalene groups per polymer chain, $M_{n,p} \cong 110$ kg/mol the number average molar mass of the copolymer **P(DMA-N1)** and $M_{n,s} \cong 10$ kg/mol the number average molar mass between two consecutive naphthalene units.

As reported in **Table 3** the fraction of elastically active chains formed in stoichiometric conditions (B/N=1) strongly increases with polymer concentration starting with a very low value (f_x=0.05) at C_p=10 wt%. In these conditions where the fraction of non-coordinated **BB** is negligible and the extrapolated fraction of di-coordinate is higher than 95 %, this means that most of the di-coordinated **BB** cross-linkers are involved into intra-chain bounds (loops) rather than inter-chain ones (bridges).

Table 3. Viscoelastic parameters of P(DMA-N1) formulations prepared with added di-blue box and studied at T=5 °C. C_p is the polymer concentration, B/N the stoichiometric ratio, G_0 the plateau modulus, τ the relaxation time, f_x the fraction of elastically active chains, x the mean number of elastically active chains per copolymer chain as defined by equations {9} and {10}, respectively, p_{inter} the fraction of interchain bonds and C_p/C^* the degree of chain overlapping.

C_p wt%	5	10				15		20	
B/N	1	0	0.5	1	1.5	1	0.5	1	1.5
G_0 Pa				612		2600	1274	6600	3300
τ (s)				0.069		0.146	0.075	0.259	0.11
f_x				0.05		0.15	0.055	0.29	0.14
x				0.59		1.65	0.61	3.14	1.57
p_{inter}				0,16		0,27	0,16	0,41	0,26

C_p/C^*	2.5	5	7.5	10

In terms of connectivity, $x \cong 0.6$ at C_p=10 wt% corresponds to the gelation regime in which all the chains do not yet participate in the elasticity of the network. Indeed, while on average there is one cross-link per chain (N_x=1) at the gel point (or percolation threshold), which marks the beginning of the gelation regime, the end of the latter takes place when almost all the chains are connected to the network. This corresponds to the beginning of the gel regime when there is on average two cross-links per chain (N_x=2 and x=1). This situation, where all the polymer chains contribute at least once to the elasticity of the gel, is typically the condition for network formation as defined by Flory ($x \geq 1$) [28]. Within the gelation regime (x<1), it is necessary to consider that the network structure is not homogeneous and this is particularly the case in the vicinity of the gel point. For x=0.6, there should be a steady state between the 3D network and a fraction of isolated chains or clusters that are dissociated from the network and that do not contribute substantially to the viscoelastic properties. By increasing the concentration, the probability to form inter-chain bridges strongly increases as shown by the variation of f_x that reaches 0.15 and 0.29 at Cp=15 and 20 wt%, respectively. At these concentrations, x is higher than 1 which means that all the chains are now connected to the network and each polymer chain contribute at least once to the elasticity. In this gel regime, x also represents the extent of the reaction (ε) that can be defined as:

$$x \cong \varepsilon = \left(C_p - C_p^c\right)\!/C_p^c \qquad \{13\}$$

where C_p^c is the polymer concentration at the gel point.

Using the x values calculated in stoichiometric conditions for C_p = 15 and 20 wt% we can extrapolate the gel point at $C_p^c \cong 5\,\text{wt\%}$, in good agreement with the former discussion on viscoelastic properties.

As shown in **Table 3**, the percentage of elastically active chains reaches 29 % at high polymer concentration (C_p=20 wt%) in stoichiometric conditions but their contribution strongly

decreases when moving away from the stoichiometry with f_x=5.5 % and 14 % for B/N=0.5 and 1.5, respectively. At this polymer concentration the number of elastically active subchains is maximum at B/N=1 (x=3.1) and it decreases progressively to x=0.6 (B/N=0.5) or 1.6 (B/N=1.5). Below the stoichiometry, the decrease of x (or f_x) is correlated with the lower amount of inter-chain bound **cross-linkers**, as most **BB** molecules form N-BB-N di-coordinates ($[NBBN]_{eq}/[N]_T \cong 0.5$ and $[N]_{eq}/[N]_T \cong 0.5$); see **Figure 4b**). Above the stoichiometry, the loss of elasticity is mainly related to the increasing number of mono-coordinate N-BB dangling groups ($[NBBN]_{eq}/[N]_T \cong 0.77$ and $[NBB]_{eq}/[N]_T \cong 0.23$). As calculated in **Figure 4b**, the fraction of di-coordinates N-BB-N ($p_{NBBN} = [NBBN]_{eq}/[N]_T$) is much higher for B/N=1.5 ($p_{NBBN} = 0.77$) compared to B/N=0.5 ($p_{NBBN} \cong 0.5$) and the same is true for the density number of elastically active chains. As discussed with the critical concentration at the gel point, calculated for stoichiometric formulations, the same procedure can be used to determine at a given polymer concentration the critical fraction of di-adduct at the gel point: $p^c_{NBBN} = [NBBN]^c_{eq}/[N]_T$. Using $x \cong \varepsilon = \left(p_{NBBN} - p^c_{NBBN} \right) / p^c_{NBBN}$ {14} with p_{NBBN}=0.92 and x=1.65 for C_p=15 wt%, or p_{NBBN}=0.96 and x=3.14 at C_p= 20 wt%, the critical conditions are obtained for $p^c_{NBBN} = 0.35$ and 0.23, respectively. As the complexation is almost quantitative at these concentrations below the stoichiometric conditions (B/N<1), this analysis allows to extrapolate the minimum amount of di-blue box to be added to the polymer solution $(B / N)^c \cong p^c_{NBBN}$ to reach the gel point.

Scaling relations

Despite the limited number of data, scaling relations can nevertheless be defined in the gelation and gel regimes where formulations demonstrate a Maxwellian behavior. Looking first at the Newtonian viscosity, the stoichiometric formulations (C_p=10 to 20 wt%) display a high concentration dependence with $\eta \approx C^\gamma_p$ with γ=5.3. This result compares relatively well,

although without a strong conclusion, with theoretical values issued from the sticky Rouse model for concentrations below the overlap concentration of the strands between stickers (C_{str}*) [31]. For **P(DMA-N1)** solutions this concentration could be estimated close to 20 wt%. The high values of the theoretical exponents that characterized this gel regime, γ=3 (3.5) and 4.2 (5.9) for Θ and good solvents, respectively, without (or with) renormalized bond lifetime, mainly result from the transformation of intramolecular bonds into intermolecular ones. Above C_{str}*, most of the bonds are assumed to be intermolecular and the concentration dependence of the viscosity becomes much weaker (γ≤1).

If we analyze similarly the concentration dependence of the plateau modulus, it comes $G_0 \approx C_p^{3.4}$ with a high scaling exponent. In the gel regime, which correspond to the situation where all the chains are involved in the network (x>1), the sticky Rouse model predicts $G_0 \approx xRTC_p/M_{n,p}$ {15}. For x=1, the plateau modulus recovers the familiar result $G_0 \approx RTC_p/M_{n,p}$ and the relaxation time is simply the sticker lifetime τ_b, or its renormalized value τ_b* as discussed previously. The variation of x is highlighted in **Figure S13** (Supporting Information) where x has been plotted versus the polymer concentration normalized by the molar fraction of di-coordinated N-BB-N $\left([NBBN]_{eq}/[N]_T = p_{NBBN} = p_{int\,ra} + p_{int\,er}\right)$ in order to take into account the real content of potential BB cross-linkers independently of the stoichiometry. A common behavior is obtained for all the formulations, regardless of the stoichiometry, with a strong concentration dependence of x ($x \approx (p_{NBBN}C_p)^{2.4}$). Similarly the logarithmic representation of the fraction of inter-chain bounds with respect to the normalized concentration (**Figure S14** in Supporting Information) demonstrates clearly the transformation from intramolecular bond into intermolecular ones: $p_{int\,er} \approx (p_{NBBN}C_p)^{1.3}$. This exponent is in good agreement with the theory of associating polymers developed by Rubinstein and Semenov [31] who predicts that below the overlap concentration of the strands

between stickers ($C_p < C_{str}{}^*$), the fraction of closed stickers that form inter-chain bonds scales as $p_{\text{inter}} \propto C_p^{\delta}$, with δ=1 and 1.6 for polymer chains in Θ and good solvents, respectively. Then, the conclusion for the strong concentration dependence of the plateau modulus is that, in the range of concentrations investigated, which is in the vicinity of the gel regime ($x \cong 1$), the elastic properties are mainly controlled by the transformation of di-coordinated BB from intra-molecular into intermolecular bounds.

As $\eta \approx C_p^{5.3}$ and $G_0 \approx C_p^{3.4}$ for stoichiometric formulations, the relaxation time of supramolecular gels varies as $\tau \propto C_p^{1.9}$. According to the sticky Rouse model, assuming un-renormalized bond lifetime (τ_b), a first elastic signature should appear above the gel point, in the gelation regime where mean-field theory applies, with a low plateau modulus $G_0 < RTC_p / M_{n,p}$ and a low relaxation time $\tau < \tau_b$ that will increase with the extent of the degree of cross-linking; i.e. the polymer concentration or the amount of connections. These parameters reach their reference values, $G_0 \approx RTC_p / M_{n,p}$ and $\tau = \tau_b$, for x=1 (N_x=2), and then the modulus increases linearly with x as underlined by equation {15}. In parallel, for x>1, the solution is expected to display at least two characteristic times: τ_b, which corresponds to the effective lifetime of a strand between cross-linkers and $\tau_{chain} = \tau_b N_x^2$, the relaxation time of the whole chain in the sticky Rouse model [65]. Nevertheless, as reported by Indei et al [33], the terminal relaxation time τ_{chain} only appears if N_x is large enough, otherwise the dynamic shear moduli are well described in terms of the Maxwell model characterized by a single relaxation time in the moderate and lower frequency regimes. This is the situation we are facing in this study, at the border between gelation (x<1) and gel (x>1) regimes, which can explain why all the formulations investigated display a single relaxation time without a clear signature of sticky Rouse dynamics. As shown in **Figure 12**, for all the formulations investigated, the relaxation time scales with the mean number of cross-links per

copolymer chain as: $\tau \approx N_x^{1.3}$. Assuming that the relaxation time is equal to the bound lifetime

τ_b when $N_x=2$ (or $x=1$), this plot makes possible to estimate the lifetime of BN association (

$\tau_b \cong 0.1$ s) and conversely the relaxation rate or dissociation rate constant ($\beta \cong 10$ s^{-1}), under

the assumption of unrenormalized bonds. A similar data treatment has been proposed by

Craig et al. for supramolecular polymer networks based on metal-ligand coordination [25]. In

this case, the dissociation rate was shown to decrease linearly with the degree of cross-linking

($\beta \approx N_x^{-1}$) and the dissociation rate of supramolecular crosslinks, was obtained by

extrapolating the relaxation rate back to the cross-link density at the gel point. The

extrapolated value was shown to be very close to the experimental dissociation rate constant

(k_d) determined from corollary NMR studies of the small molecule supramolecular motif.
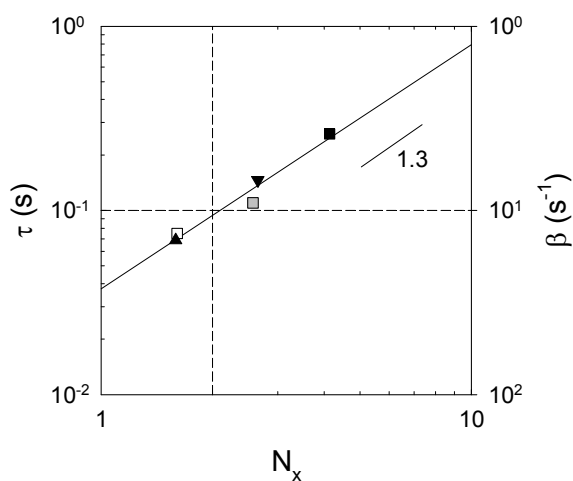

Figure 12

Variation of the relaxation time (τ) and the relaxation rate (β) as a function of the mean number of cross-links per copolymer chain (N_x). Black symbols hold for stoichiometric conditions (B/N=1), grey for B/N=1.5 and white for B/N=0.5: P(DMA-N1) at Cp= 10 wt% (▲), 15 wt% (▼) and 20 wt%(■■□).

This scaling behaviour ($\beta \approx N_x^{-1}$ or $\tau \approx N_x$), different from the sticky Rouse relaxation well

above the gel point ($\tau \approx N_x^2$), has been reported with other supramolecular polymer networks

based on metal-ligand coordination [34] and host-guest complexation [45] and compared with

the transient network model developed by Jongschaap and co-workers [32]. According to this

model of polymer chain with multiple stickers that consider the stress release only from

terminal subchains, the mean relaxation time of the network grows roughly in a linear way

with the number of physical cross-links that have to break for such a process. In the present work, the log-log plot of the relaxation time as a function of the mean number of cross-links per copolymer chain (**Figure 12**) shows an intermediate exponent: $\tau \approx N_x^{1.3}$. In these conditions we are more incline to correlate our experimental results with the theoretical work of Indei [33] which predicts the observation of two distinguishable relaxation processes τ_{chain} and τ_b only if N_x is large enough. Close to the gel regime, the Rouse relaxation time of the chain is not clearly observable and we postulate that the relaxation time extrapolated from the Maxwell behavior is intermediate between these two characteristic times. Another hypothesis, that was pointed out by Olsen et al [35] in a recent work based on very similar supramolecular polymer hydrogels, is that the increase of the relaxation time with polymer concentration would originate from the increasing time needed to have an efficient exchange (i.e. allowing for chain relaxation). Nevertheless, whatever is the apparent scaling coefficient for the relation and the exact reason for its concentration dependence, the extrapolation of the relaxation time back to the gel transition is an interesting way to get access to the lifetime of a supramolecular bond. The extrapolation of τ_b, either at the gel point ($N_x=1$) or at the beginning of the gel regime ($N_x=2$) remains an open question.

CONCLUSION

The main goal of this work was to develop new supramolecular polymer hydrogels based on the complex formation between electron donor and acceptor molecules; namely naphthalene and CBPQT^{4+}. The thermodynamic analysis of the association constant between blue box molecules and PDMA chains lightly modified with naphthalene groups has evidenced strong interactions with almost full conversion of the complex in the concentration range studied and for temperatures typically below 40 °C. The addition of a di-blue box cross-linker to the semi-dilute un-entangled copolymer solution is responsible for the sol/gel transition above the

overlap concentration of polymer chains. All supramolecular hydrogels are well described in terms of the Maxwell model characterized by a plateau modulus and a single relaxation time. While the temperature has been shown to have a very weak impact on G_0, the temperature dependence of the relaxation time of stoichiometric systems follows an Arrhenius variation characterized by a high activation energy $E_\tau = E_\eta = 105$ kJ/mol. From a whole set of formulations prepared with different polymer concentration and B/N stoichiometry, a strong overturn from intra-chain loops to inter-chain bridges was emphasized with increasing concentration ($p_{\mathrm{int}\,er} \propto C_p^{1.3}$). The fraction of effective supramolecular cross-linkers and the lifetime of supramolecular bonds are clearly the key parameters of these supramolecular hydrogels as they also impact the relaxation time of the polymer network. The extrapolation of the latter back to the gel transition (x=1) allows to estimate the lifetime of the complex and its dissociation constant $k_d \cong 10$ s^{-1}. Complementary experiments are needed to get further insight into the dynamics of supramolecular systems prepared from un-entangled polymer solutions and more generally to get a better understanding of dynamics: from host/guest molecules to polymer networks. In the general framework of supramolecular gels, di-CBPQT^{4+} cross-linkers could provide a very powerful platform as they can be used with other macromolecular architectures, like telechelic or star-like polymers, other π-electron donors like tetrathiafulvalene, as well as in organic media if changing the Cl$^-$ anions of the CBPQT^{4+} by PF_6^-.

REFERENCES

1. D. N. Schulz, J. E. Glass, *Polymers as rheology modifiers*, ACS symposium series, vol. 467, Washington DC, 1991.

2. T. Annable, R. Buscall, R. Ettelaie, D. Whittlestone, *J. Rheol.*, 1993, **37**, 695-726.

3. E. J. Regalado, J. Selb, F. Candau, *Macromolecules*, 1999, **32**, 8580-8588.

4. G. Bokias, D. Hourdet, I. Iliopoulos, *Macromolecules*, 2000, **33**, 2929-2935.

5. D. Hourdet, J. Gadgil, K. Podhajecka, M. V. Badiger, A. Brulet, P. P. Wadgaonkar, *Macromolecules*, 2005, **38**, 8512-8521.

6. G. Pouliquen, C. Tribet, *Macromolecules*, 2007, **39**, 373-383.

7. I. Dimitrov, B. Trzebicka, A. H. E. Müller, A. Dworak, C. B. Tsvetanov, *Prog. Polym. Sci.*, 2007, **32**, 1275-1343.

8. K. C. Taylor, H. A. Nasr-El-Din, *J. Petrol. Sci. Eng.*, 1998, **19**, 265-280.

9. N. Bhattarai, H. R. Ramay, J. Gunn, F. A. Matsen, M. Zhang, *J. Control. Release*, 2005, **103**, 609-624.

10. D. Cohn, A. Sosnik, S. Garty, *Biomacromolecules*, 2005, **6**, 1168-1175.

11. E. Siband, Y. Tran, D. Hourdet, *Macromolecules*, 2011, **44**, 8185-8194.

12. P. Schattling, F. D. Jochum, P. Theato, *Polym. Chem.*, 2014, **5**, 25-36.

13. P. Alexandridis, T. A. Hatton, *Colloids Surf. A: Physicochem. Eng. Asp.*, 1995, **96**, 1-46.

14. F. Petit, I. Iliopoulos, R. Audebert, S. Szönyi, *Langmuir*, 1997, **13**, 4229-4233.

15. A. Tripathi, K. C. Tam, G. H. McKinley, *Macromolecules*, 2006, **39**, 1981-1999.

16. G. Whitesides, J. Mathias, C. Seta, *Science*, 1991, **254**, 1312–1319.

17. D. Reinhoudt, J. Atwood, J. Lehn, *Comprehensive Supramolecular Chemistry*, Pergamon Press, 1996.

18. T. Aida, E. W. Meijer, S. I. Stupp, *Science*, 2012, **335**, 813-817.

19. S. L. Li, T. Xiao, C. Lin, L. Wang, *Chem. Soc. Rev.*, 2012, **41**, 5950-5968.

20. S. Seiffert, J. Sprakel, *Chem. Soc. Rev.*, 2012, **41**, 909-930.

21. E. A. Appel, J. del Barrio, X. J. Loh, O. A. Scherman, *Chem. Soc. Rev.*, 2012, **41**, 6195-6214.

22. M. Anthamatten, *Adv. Polym. Sci.*, 2015, **268**, 47-99.

23. M. J. Webber, E. A. Appel1, E. W. Meijer, R. Langer, *Nat. Mater.*, 2015, **15**, 13-26.

24. W. C. Yount, D. M. Loveless, S. L. Craig, *Angew. Chem.*, 2005, **117**, 2806-2808.

25. W. C. Yount, D. M. Loveless, S. L. Craig, *J. Am. Chem. Soc.*, 2005, **127**, 14488-14496.

26. D. Xu, J. L. Hawk, D. M. Loveless, S. L. Jeon, S. L. Craig, *Macromolecules*, 2010, **43**, 3556-3565.

27. D. Xu, S. L. Craig, *Macromolecules*, 2011, **44**, 5465-5472.

28. P. J. Flory, *Principles of Polymer Chemistry*, Cornell University Press, Ithaca, NY, 1953.

29. M. E. Cates, *Macromolecules*, 1987, **20**, 2289-2296.

30. S. P. Obukhov, M. Rubinstein, R. H. Colby, *Macromolecules*, 1994, **27**, 3191-3198.

31. M. Rubinstein, A. N. Semenov, *Macromolecules*, 2001, **34**, 1058-1068.

32. R. J. J. Jongschaap, R. H. W. Wientjes, M. H. G. Duits, J. Mellema, *Macromolecules*, 2001, **34**, 1031-1038.

33. T. Indei, J.-I. Takimoto, *J. Chem. Phys.*, 2010, **133**, 194902.

34. S. Hackelbusch, T. Rossow, P. van Assenbergh, S. Seiffert, *Macromolecules*, 2013, **46**, 6273-6286.

35. S. Tang, B. D. Olsen, *Macromolecules*, 2016, **49**, 9163-9175.

36. N. Holten-Andersen, M. J. Harrington, H. Birkedal, B. P. Lee, P. B. Messersmith, K. Y. C. Lee, J. H. Waite, *Proc. Natl. Acad. Sci. U. S. A.*, 2011, **108**, 2651-2655.

37. S. C. Grindy, R. Learsch, D. Mozhdehi, J. Cheng, D. G. Barrett, Z. Guan, P. B. Messersmith, N. Holten-Andersen, *Nat. Mater.*, 2015, **14**, 1210-1216.

38. J. Brassinne, J. F. Gohy, C. A. Fustin, *ACS Macro Lett.*, 2016, **5**, 1364-1368.

39. A. Harada, Y. Takashima, H. Yamaguchi, *Chem. Soc. Rev.*, 2009, **38**, 875–882.

40. J. Li, X. J. Loh, *Adv. Drug Delivery Rev.*, 2008, **60**, 1000–1017.

41. A. Charlot, R. Auzely-Velty, M. Rinaudo, *J. Phys. Chem. B*, 2003, **107**, 8248-8254.

42. X. Guo, J. Wang, L. Li, D.-T. Pham, P. Clements, S. F. Lincoln, B. L. May, Q. Chen, L. Zheng, R. K. Prud'homme, *J. Polym. Sci., Part B: Polym. Phys.*, 2010, **48**, 1818-1825.

43. O. Kretschmann, S. W. Choi, M. Miyauchi, I. Tomatsu, A. Harada, H. Ritter, *Angew. Chem., Int. Ed.*, 2006, **45**, 4361-4365.

44. A. Day, A. P. Arnold, R. J. Blanch, B. Snushall, *J. Org. Chem.*, 2001, **66**, 8094-8100.

45. E. A. Appel, F. Biedermann, U. Rauwald, S. T. Jones, J. M. Ayed, O. A. Scherman, *J. Am. Chem. Soc.*, 2010, **132**, 14251-14260.

46. L. Sambe, F. Stoffelbach, K. Poltorak, J. Lyskawa, A. Malfait, M. Bria, G. Cooke, P. Woisel, *Macromol. Rapid Commun.*, 2014, **35**, 498-504

47. C. Cheng, T. Cheng, H. Xiao, M. D. Krzyaniak, Y. Wang, P. R. McGonigal, M. Frasconi, J. C. Barnes, A. C. Fahrenbach, M. R. Wasielewski, W. A. Goddard, J. F. Stoddart, *J. Am. Chem. Soc.*, 2016, **138**, 8288-8300.

48. M. Bria, J. Bigot, G. Cooke, J. Lyskawa, G. Rabanic, V. M. Rotellod, P. Woisel, *Tetrahedron*, 2009, **65**, 400-407.

49. I. R. Fernando, M. Frasconi, Y. Wu, G.-G. Liu, M. R. Wasielewski, W. A. Goddard III, J. F. Stoddart, *J. Am. Chem. Soc.*, 2016, **138**, 10214-10225.

50. P. R. Ashton, R. Ballardini, V. Balzani, M. Belohradsky, M. T. Gandolfi, D. Philp, L. Prodi, F. M. Raymo, M. V. Reddington, N. Spencer, J. F. Stoddart, M. Venturi, D. J. Williams, *J. Am. Chem. Soc.*, 1996, **118**, 4931-4951.

51. G. Cooke, J. F. Garety, S. G. Hewage, B. J. Jordan, G. Rabani, V. M. Rotello, P. Woisel, *Org. Lett.*, 2007, **9**, 481-484.

52. M. Bria, G. Cooke, A. Cooper, J. F. Garety, S. G. Hewage, M. Nutley, G. Rabanib, P. Woisel, *Tetrahedron Lett.*, 2007, **48**, 301-304.

53. B. Yeniad, K. Ryskulova, D. Fournier, J. Lyskawa, G. Cooke, P. Woisel, R. Hoogenboom, *Polym. Chem.*, 2016, **7**, 3681–3690.

54. K. Belal, F. Stoffelbach, J. Lyskawa, M. Fumagalli, D. Hourdet, A. Marcellan, L. De Smet, V. R. de la Rosa, G. Cooke, R. Hoogenboom, P. Woisel, *Angew. Chem., Int. Ed.*, 2016, **55**, 13974-13978.

55. J. Bigot, B. Charleux, G. Cooke, F. Delattre, D. Fournier, J. Lyskawa, L. Sambe, F. Stoffelbach, P. Woisel, *J. Am. Chem. Soc.*, 2010, **132**, 10796-10801.

56. J. Bigot, M. Bria, S. T. Caldwell, F. Cazaux, A. Cooper, B. Charleux, G. Cooke, B. Fitzpatrick, D. Fournier, J. Lyskawa, M. Nutley, F. Stoffelbach, P. Woisel, *Chem. Commun.*, 2009, **35**, 5266-5268.

57. L. Sambe, V. R. de La Rosa, K. Belal, F. Stoffelbach, J. Lyskawa, F. Delattre, M. Bria, G. Cooke, R. Hoogenboom, P. Woisel, *Angew. Chem.*, 2014, **53**, 5044-5048.

58. C.-H. Sue, S. Basu, A. C. Fahrenbach, A. K. Shveyd, S. K. Dey, Y. Y. Botros, J. F. Stoddart, *Chem. Sci.*, 2010, **1**, 119-125.

59. A. Malfait, F. Coumes, D. Fournier, G. Cooke, P. Woisel, *Eur. Polym. J.*, 2015, **69**, 552-558.

60. K. Belal, S. Poitras-Jolicoeur, J. Lyskawa, G. Pembouong, G. Cooke, P. Woisel, F. Stoffelbach, *Chem. Commun.*, 2016, **52**, 1847-1850.

61. R. Colby, *Rheol. Acta*, 2010, **49**, 425-442.

62. T. Rossow, S. Seiffert, *Polym.Chem.*, 2014, **5**, 3018-3029.

63. M. Rubinstein, A. R. Semenov, *Macromolecules*, 1998, **31**, 1386-1397.

64. E. A. Appel, R. A. Forster, A. Koutsioubas, C. Toprakcioglu, O. A. Scherman, *Angew. Chem., Int. Ed.*, 2014, **53**, 10038-10043.

65. Q. Chen, C. Huang, R. A. Weiss, R. H. Colby, *Macromolecules*, 2015, **48**, 1221-1230.

Table of Contents Entry

Supramolecular polymer hydrogels induced by host-guest interactions with di-[cyclobis(paraquat-*p*-phenylene)] cross-linkers: from molecular complexation to viscoelastic properties

Matthieu Fumagalli[1,2], Khaled Belal[3], Hui Guo[1,2], François Stoffelbach[4],

Graeme Cooke[5], Alba Marcellan[1,2], Patrice Woisel[3*] and Dominique Hourdet[1,2*]

Formation of a supramolecular polymer network induced by host-guest interactions between di-[cyclobis(paraquat-*p*-phenylene)], BB, and poly(*N,N*-dimethylacrylamide-co-naphthalene acrylamide), P(DMA-N1).